RESEARCH FRONT

CSIRO PUBLISHING

Aust. J. Chem. **2014**, *67*, 435–443
http://dx.doi.org/10.1071/CH13480

Full Paper

Description of Bond Pseudorotation, Bond Pseudolibration, and Ring Pseudoinversion Processes Caused by the Pseudo-Jahn–Teller Effect: Fluoro Derivatives of the Cyclopropane Radical Cation

Wenli Zou[A] *and Dieter Cremer*[A,B]

[A]Department of Chemistry, Southern Methodist University, 3215 Daniel Ave, Dallas, Texas 75275-0314, USA.
[B]Corresponding author. Email: dieter.cremer@gmail.com

Curvilinear coordinates are used to describe the molecular geometry and the pseudo-Jahn–Teller surface of F-substituted cyclopropane radical cations using the equation-of-motion coupled cluster EOMIP-CCSD/cc-pVTZ approach. The monofluoro derivative **2** undergoes bond pseudolibration (incomplete bond pseudorotation) between two symmetry-equivalent biradicaloid forms separated by a barrier of 2.2 kcal mol^{-1} (1 kcal mol^{-1} = 4.186 kJ mol^{-1}) at low temperature. Bond pseudorotation and ring pseudoinversion have barriers of 12.1 and 16.5 kcal mol^{-1} respectively. The relative energies of **2** are affected by the distribution of the positive charge in the C_3 ring and the formation of a CF bond with partial π character. There is a change of the CF bond length from 1.285 to 1.338 Å along the bond pseudorotation path. The changes of the CF bond outweigh the deformation effects of the C_3 ring; however, both are a result of the pseudo-Jahn–Teller effect according to an $(A' + A'') \otimes (a' + a'')$ interaction. For the pentafluoro derivative **3** of the cyclopropane radical cation, bond pseudorotation has a barrier of 16.3 kcal mol^{-1} whereas ring pseudoinversion is hindered by a barrier of 21.7 kcal mol^{-1}. Radical cation **3** is the first example of a trimethylene radical cation.

Manuscript received: 11 September 2013.
Manuscript accepted: 16 October 2013.
Published online: 28 November 2013.

Introduction

The Jahn–Teller effect (JTE) leads to a distortion of high-symmetry structures of polyatomic molecules with electronic degenerate states.[1–3] The pseudo-JTE (PJTE) occurs when an excited state of low energy interacts via vibronic coupling with the ground state and this interaction also leads to the distortion of a high-symmetry form.[3,4] Hence, the PJTE is caused by a pseudo-degeneracy of ground and low-lying excited states. This has led to the formulation of a structural instability theorem:[4] molecules tend to avoid degeneracy or pseudo-degeneracy by means of symmetry-breaking, i.e. deforming from a structure of higher symmetry to a structure of lower symmetry.

Most of the recent work has focussed on how the JTE and PJTE influence structure and stability of high-symmetry molecules with (quasi-)degenerate states.[3] However, a typical (P) JT-distortion can also trigger dynamic processes of which bond pseudorotation is the most fascinating one.[5–7]

As the term suggests, this dynamic process implies a cyclic exchange of bonds in a JT- or PJT-unstable ring system, thus conveying the impression of a rotation of the bonds around the periphery of the ring molecule without generating an angular momentum.

In most cases, bond pseudorotation has been investigated for highly symmetric systems with small pseudorotation barriers leading at room temperature to molecules without a specific structure.[6,7] In the present work, we will extend our studies to molecules of lower symmetry so that state degeneracy is no longer an issue, where however a PJTE becomes possible. We will show that in these cases, bond pseudorotation is still possible, where however because of the lower symmetry of the PJT surface, new dynamic processes such as incomplete bond pseudorotation or state-flipping via bond exchange will result.

When applying internal coordinates or Cartesian coordinates, a JT or PJT surface is difficult or impossible to calculate. In recent work, we have demonstrated[6,7] that by using a well-defined set of curvilinear coordinates, JTE and PJTE distortions can be quantitatively described, JT or PJT surfaces can be calculated, and the description of dynamic processes such as bond pseudorotation becomes feasible.[6,7] In the present work, we will use curvilinear coordinates for the description of the JT or PJT surface of the cyclopropane radical cation (**1**), its monofluoro derivative (**2**), and its pentafluoro derivative (**3**, see Fig. 1). We will demonstrate how the PJTE strongly influences the properties and the dynamic behaviour of the latter two radical cations.

The results of this work are presented in the following way. In the Computational Methods section, the mathematical basis of the curvilinear coordinates is sketched and the quantum chemical methods used in this work are described. In the Results and Discussion section, the JT and PJT surfaces of **1**, **2**, and **3** are described and discussed. In the last section, conclusions and an outlook on future work are given.

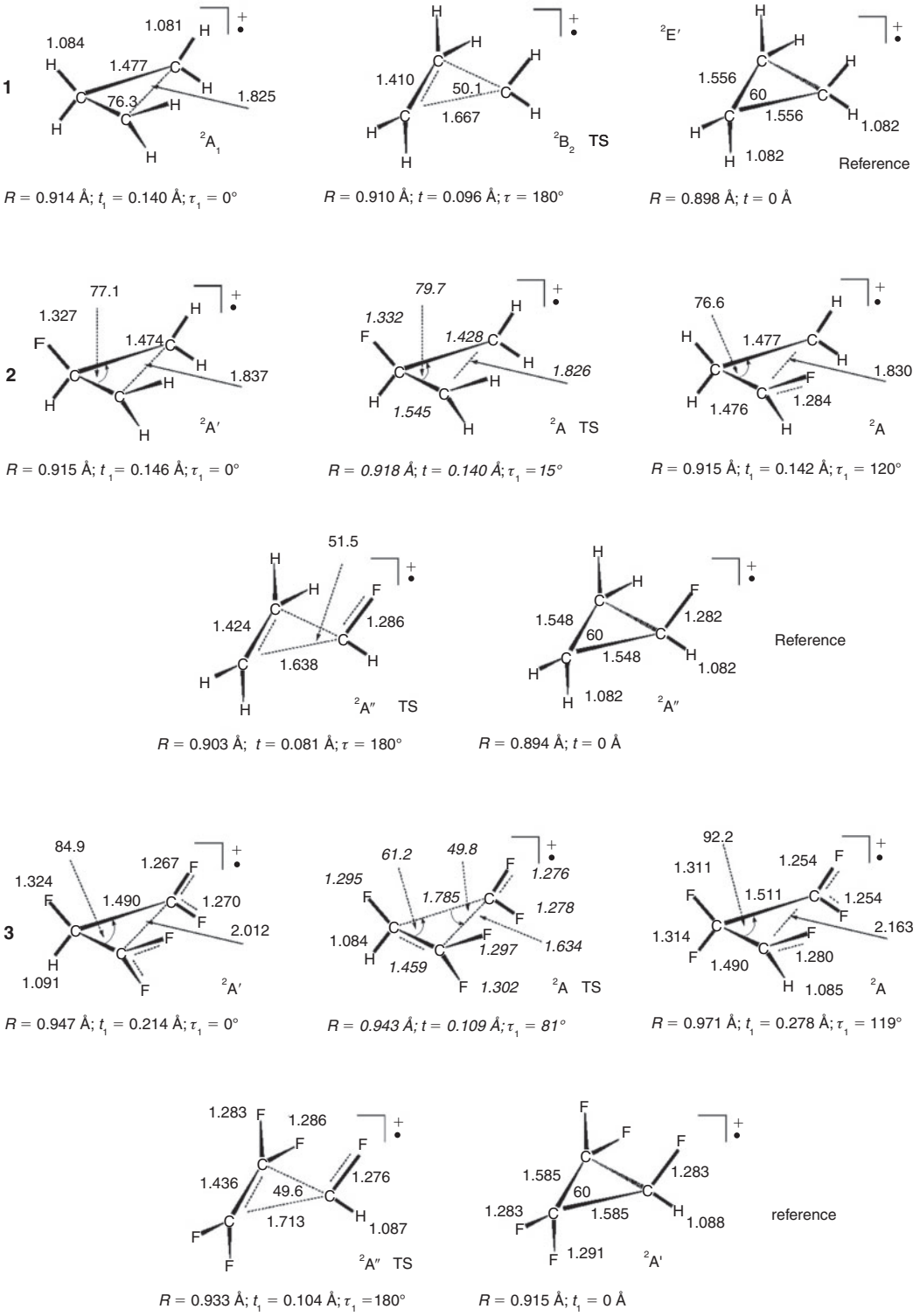

Fig. 1. Cyclopropane radical cations **1**, **2**, and **3** investigated in this work. EOM-CCSD/cc- pVTZ (normal print) and UB3LYP/cc-pVTZ geometries (italics). Bond lengths in Å and bond angles in degrees. For the definition of the curvilinear coordinates R, t_1, and τ_1, see text.

Computational Methods

For the purpose of deriving the PJT deformations of **2** and **3**, we use the curvilinear coordinates for planar ring systems derived recently.[6,7] Each planar monocyclic molecule carries out 2N – 3 (N: number of ring atoms) in-plane normal mode vibrations, which are best characterized using an N-membered polygon (*N-gon*) with D_{Nh} symmetry. Each ring carries out a breathing vibration, which preserves the overall symmetry, but however changes the ring bond lengths. Hence, 2N – 4 vibrational modes remain, which lead to ring deformations and lower the ring symmetry. As shown by Zou and Cremer,[6,7] these vibrations can be grouped into N – 2 pairs because they are either members of the same E-symmetrical vibration or can be grouped together as they lead to similarly deformed *N-gon*s. This is the case for

the b_{1u}- and b_{2u}-symmetrical vibration of the 6-gon, which both lead to a D_{3h}-symmetrical distortion and therefore are taken together as one vibrational pair.[6,7]

By assigning a finite displacement to each vibration, a set of deformation vectors results by which an *N-gon* is deformed in N – 2 characteristic ways. A mathematical equation of the deformation vectors is derived by utilizing group theory and the character table of the D_{Nh} point group.[6] Each of them is spanned by two unit vectors defined in a suitable in-plane coordinate system. Zou and Cremer have shown that the weighting coefficients of the unit vectors can be transformed into curvilinear coordinates by a Fourier transformation.[6,7] Hence, for each pair of vibrational modes (the normal mode vectors are frozen for fixed-displacement values), two curvilinear coordinates result, which span a two-dimensional deformation space. One is a deformation amplitude t_n (with $n = 1, 2, \ldots, N - 2$ corresponding to deformation pair n), which (after appropriate normalization) defines the degree of deformation. The second curvilinear coordinate presents a deformation phase angle τ_n, which specifies the mode of deformation.

One can define for each two-dimensional deformation subspace two forms, e.g. for $\tau_n = 0°$ and $t_n =$ constant the first and for $\tau_n = 180°$ and $t_n =$ constant the second, and then represent any other form with an arbitrary τ_n and t_n as a linear superposition of the two basis forms of the subspace in question. In the case of the three-membered ring, there is only one two-dimensional deformation space spanned by t_1 and τ_1. In Fig. 2 (top), selected three-ring forms are shown for a deformation amplitude $t_1 = 0.1$ Å every 15° for τ_1 from 0° to 360°. At the origin of the two-dimensional deformation space (i.e. $t_1 = 0$ Å), the undeformed D_{3h}-symmetrical three-membered ring is located.

The total deformation space of a three-membered ring has the dimension 3 because the two-dimensional deformation space is augmented by a one-dimensional breathing space. If the D_{3h}-symmetrical form of a given system is defined by a circumscribed circle with radius R_0, then any deviation from R_0 in the course of a deformation is given by the amplitude $t_0 = R - R_0$ where R is the radius of the circle of the deformed three-membered ring. The total deformation amplitude T of a deformed three-membered ring is given by amplitudes t_0 and t_1 according to:

$$T^2 = t_0^2 + t_1^2 \qquad (1)$$

The total deformation amplitude T can be used to determine the contribution of each deformation mode $n = 0,1$ to the total ring deformation (given in percentage) utilizing the ratio t_n^2/T^2. The ratios are useful for identifying the influence of different physical effects on the electronic structure of the ring molecule.

In previous work, we developed algorithms that convert Cartesian coordinates and internal coordinates into curvilinear coordinates and vice versa.[6] Programs have been written to carry out geometry optimization and frequency calculations in terms of curvilinear coordinates without ever referring to bond lengths or bond angles.[7] All calculations based on curvilinear coordinates and presented in the current work have been carried out with the program *RING*,[8] which is a part of the *ab initio* program *COLOGNE2013*.[9]

A dual-level approach was applied in this work to calculate the deformation space of cyclopropane radical cations **1**, **2**, and **3**. Preliminary geometry optimizations were carried out with B3LYP[10,11] and Dunning's cc-pVTZ basis set.[12] A total of 32

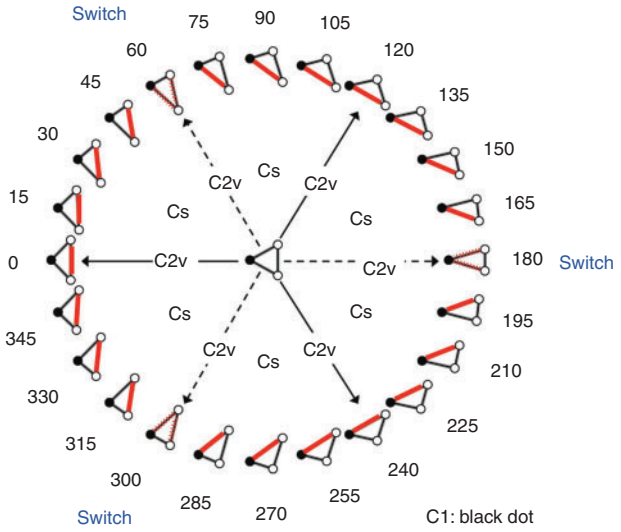

Fig. 2. Bond pseudorotation cycle of a 3-gon. The deformed ring forms are shown for a fixed value of t_1 and pseudorotation phase angle τ_1 increasing in steps of 15° from 0° to 360°. The position of atom 1 is indicated by a black dot (clockwise numbering of ring atoms). The basis forms are given by $\tau_1 = 0°$ and 60°. They are formed every 120°. The red bond rotates once around the ring for a whole pseudorotation itinerary. At 60°, 180°, and 300°, the red bond switches from one side of the ring to the other.

different cyclopropane radical cation forms of **1**, 32 of **2**, and 38 of **3**, preferentially located along the bond pseudorotation path and other predefined positions of the JT- or PJT-deformation surface were calculated. This required that amplitude t_1 and phase angle τ_1 were fixed at specific values and the remaining curvilinear coordinates and substituent coordinates were optimized. It is noteworthy that this cannot be done by using Cartesian or internal coordinates because, for example, fixing any pair of internal coordinates does not specify a ring deformation in a systematic way. Hence, the curvilinear coordinates used in this work together with the geometry optimization and vibrational frequency programs based on them provide the only way for a systematic study of JT and PJT surfaces irrespective of the size, symmetry, and degree of substitution of the investigated ring system.

In the second step of the dual-level approach, energies and geometries were redetermined at the higher levels of theory because JT or PJT systems are typical multireference problems and cannot be expected to be reliably described at the density functional theory (DFT) level. Therefore, we employed unrestricted coupled cluster theory with all single (S) and double (D) excitations and a perturbative treatment of triple (T) excitations, i.e. UHF-CCSD(T)[13] to get a more reliable description of the geometry of **1**. Results were then refined by carrying out MR-AQCC (multireference averaged quadratic couple cluster)[14] calculations in the case of **1** and EOMIP-CCSD (equation-of-motion ionization potential coupled cluster theory in the single and double excitations approximation) in the case of **1**, **2**, and **3**.[15–17] The MR-AQCC(5,6)/cc-pVTZ calculations were performed using a two-state averaging procedure and a CASSCF reference function with a five-electron, six-orbital active space. Utilizing the EOMIP-CCSD method, the geometries of **1**, **2**, and **3** were reoptimized. All high-level calculations were carried out with the cc-pVTZ basis set.[12]

The potential energy function of the JT or PJT surface was expressed in the form of a truncated power series for the

deformation amplitudes t_n and in the form of a Fourier expansions for the phase angle τ_n:

$$\begin{aligned} V(t_n,\tau_n) = {} & V_0 + V_{10}t_n + V_{20}t_n^2 + V_{30}t_n^3 + V_{40}t_n^4 \\ & + (V_{11}t_n + V_{21}t_n^2 + V_{31}t_n^3 + V_{41}t_n^4)cos\tau_n \\ & + (V_{12}t_n + V_{22}t_n^2 + V_{32}t_n^3 + V_{42}t_n^4)cos2\tau_n \\ & + (V_{13}t_n + V_{23}t_n^2 + V_{33}t_n^3 + V_{43}t_n^4)cos3\tau_n \end{aligned} \quad (2)$$

where $n = 1$ for the radical cations investigated in this work. V_0 is the energy of the D_{3h}-symmetrical reference form and the dependence on R has been dropped because in all cases investigated, t_0 changes by less than 1.5×10^{-2} Å. The subscripts of the potential coefficients V indicate (in the first position) the value of n by position (t_1: position 1), the power of t_n by giving the relevant exponent, and (in the second position) the multiplicity m of the potential via cos m τ_n. For example, V_{22} is the coefficient of the term t_1^2 cos 2 τ_1.

Beside using the quantum chemical program package *COLOGNE2013*, the programs *CFOUR*[18] and *MOLPRO*[19] were used for the high-level coupled-cluster calculations.

Results and Discussion

In Fig. 1, the molecular geometries calculated at the stationary points are summarized. In Table 1, the corresponding relative energies and deformation coordinates are listed obtained at the EOMIP-CCSD, MR-AQCC or UB3LYP levels of theory. The analytical form of the JT or PJT surface is given in Table 2. Although some of the results for the parent molecule **1** were published previously,[6] the revised EOMIP-CCSD results are needed as reference for the fluoro-substituted systems and will be shortly discussed in the following.

*Cyclopropane Radical Cation (**1**)*

In Fig. 3, the two antisymmetric Walsh orbitals of the D_{3h}-symmetrical cyclopropane radical cation are shown. These are degenerate and occupied by just three electrons, which implies a Jahn–Teller unstable $^2E'$ state with distinct multireference character. A JT distortion of e'-symmetry leads to a stabilization of the $^2E'$ state, which adopts a C_{2v}-symmetrical form as shown on the right and the left of Fig. 3. The JT

Table 2. Analytical form of the Jahn–Teller (JT) or pseudo-JT (PJT) surface

Molecule	Coefficients							
$C_3H_6^+$ **1**	V_{20}	−392.49	V_{40}	14404.53	V_{23}	0.72	V_{43}	−5593.03
	Other coefficients are zero because of symmetry							
$C_3H_5F^+$ **2**	V_{10}	−181.58	V_{11}	168.84	V_{12}	37.42	V_{13}	69.37
	V_{20}	537.08	V_{21}	−1858.96	V_{22}	−298.85	V_{23}	−950.20
	V_{30}	2415.40	V_{31}	8419.44	V_{32}	1611.40	V_{33}	2920.28
	V_{40}	−6906.48	V_{41}	−13660.01	V_{42}	−3316.06	V_{43}	−4138.76
$C_3F_5H^+$ **3**	V_{10}	−179.42	V_{11}	−115.30	V_{12}	34.14	V_{13}	15.48
	V_{20}	857.37	V_{21}	997.09	V_{22}	−589.90	V_{23}	−351.86
	V_{30}	−1729.90	V_{31}	−3554.05	V_{32}	2803.27	V_{33}	729.16
	V_{40}	2630.00	V_{41}	4297.89	V_{42}	−3869.01	V_{43}	−1631.85

Table 1. Energies and deformation coordinates of cyclopropane radical cations 1, 2, and 3

State	Symmetry	Method	Energy [kcal mol^{-1}]	R [Å]	T [Å]	t_0 [Å]	t_1 [Å]	τ_1 [°]
$C_3H_6^+$ **1**								
$^2A_1$ (global min)	C_{2v}	EOMIP-CCSD	0.00	0.9140	0.1404	0.0156	0.1395	0
		MRAQCC	0.00	0.9181	0.1497	0.0179	0.1486	0
$^2B_2$ (TS)	C_{2v}	EOMIP-CCSD	2.10	0.9104	0.0970	0.0120	0.0963	180
		MRAQCC	2.39	0.9134	0.1005	0.0132	0.0996	180
^{2}E′ (max)	D_{3h}	EOMIP-CCSD	20.26	0.8984			0	
		MRAQCC	21.44	0.9002			0	
$C_3H_5F^+$ **2**								
^2A (global min)	C_1	B3LYP	0.00	0.9301	0.1899	0.0354	0.1866	119
		EOMIP-CCSD	0.00	0.9146	0.1435	0.0208	0.1420	120
$2A''$ (TS)	C_s	B3LYP	3.65	0.9076	0.0874	0.0129	0.0864	180
		EOMIP-CCSD	2.24	0.9029	0.0810	0.0091	0.0805	180
$2A'$ (local min)	C_s	B3LYP	11.99	0.9221	0.1704	0.0274	0.1682	0
		EOMIP-CCSD	11.88	0.9147	0.1473	0.0209	0.1458	0
^2A (TS)	C_1	B3LYP	12.20	0.9180	0.1423	0.0233	0.1404	15
		EOMIP-CCSD[B]	11.99	0.9180	0.1423	0.0233	0.1404	15
$2A''$ (max)[A]	C_s	B3LYP	18.03	0.8947			0	
		EOMIP-CCSD	16.49	0.8938			0	
$C_3F_5H^+$ **3**								
$2A'$ (global min)	C_s	B3LYP	0.00	0.9889	0.3757	0.0678	0.3695	0
		EOMIP-CCSD	0.00	0.9471	0.2168	0.0322	0.2144	0
$2A$ (local min)	C_1	B3LYP	6.49	0.9962	0.3686	0.0751	0.3609	119
		EOMIP-CCSD	4.98	0.9709	0.2836	0.0560	0.2780	119
$2A$ (TS)	C_1	B3LYP	16.95	0.9432	0.1113	0.0221	0.1091	81
		EOMIP-CCSD[B]	11.08	0.9432	0.1113	0.0221	0.1091	81
$2A''$ (TS)	C_s	B3LYP	22.81	0.9486	0.1193	0.0275	0.1161	180
		EOMIP-CCSD	16.26	0.9327	0.1051	0.0178	0.1036	180
$2A'$ (max)[A]	C_s	B3LYP	27.89	0.9211			0	
		EOMIP-CCSD	21.71	0.9149			0	

[A]The C_3 ring is constrained to D_{3h} symmetry.
[B]Calculated at the B3LYP geometry.

deformation can generate a biradicaloid form with a long C2C3 interaction (henceforth, we call atoms such as C2 and C3 terminal atoms for reasons of simplicity). Accordingly, the b_2-symmetrical molecular orbital (MO) is stabilized relative to the a_1-symmetrical MO and a $^2A_1$ state results (see Fig. 3, left side). However, if the distortion implies the partial removal of a methylene group from the remaining ethene base, a structure similar to an ethene–methylene π-complex results, for which the (stabilized) a_1-symmetrical MO is energetically below the (destabilized) b_2-symmetrical MO, thus yielding a $^2B_2$ ground state.

This is the traditional presentation of the JTE in **1** where, however, an important aspect is not considered. As shown in Fig. 2, the two-dimensional space spanned by the curvilinear coordinates t_1 and τ_1 hosts an infinite number rather than just two JT distorted forms. To identify the most stable of the JT forms of **1** and possible interconversion modes between them, one has to determine major parts of the JT deformation surface (JT surface).[6]

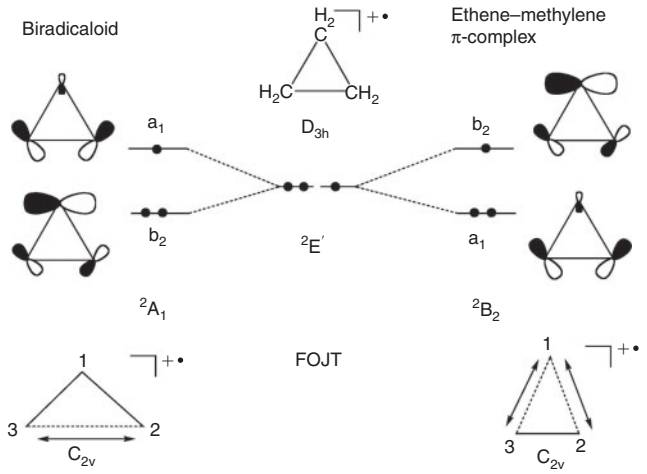

Fig. 3. Highest occupied molecular orbitals (MOs) of different forms of the cyclopropane radical cation **1**. Symmetry of the MOs, the corresponding ground state, and the deformation of the ring is given. FOJT: first-order Jahn–Teller effect.

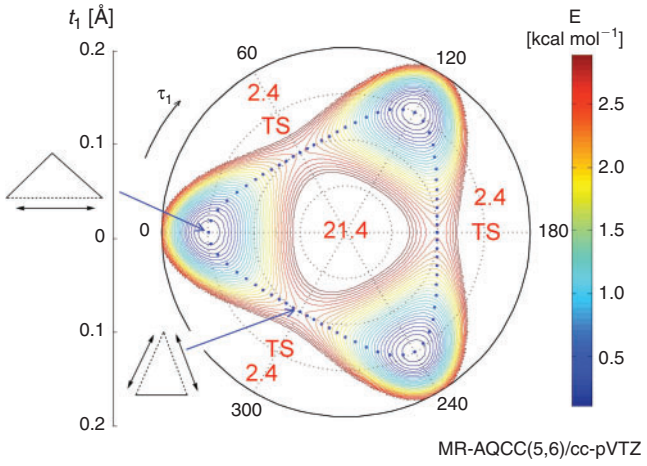

Fig. 4. Contourline diagram of the Jahn–Teller surface of the cyclopropane radical cation (**1**). The MR-AQCC energies of biradicaloid and ethene–methylene π-complex forms are given. The dotted blue line indicates the bond pseudorotation path.

In Fig. 4, a contour line diagram of the C_3-symmetrical surface is shown where the variation of the energy is given by a colour code. At the centre of the diagram ($t_1 = 0°$), there is an energy maximum of 21.4 kcal mol^{-1}, which is the position of the JT-unstable D_{3h}-symmetrical form. There are three symmetry-equivalent minima ($\Delta E = 0$ kcal mol^{-1}) at $\tau_1 = 0°$, 120°, and 240°, which are occupied by the biradicaloid forms of **1** (see Fig. 4). These forms can convert into each other by following the dotted path on the JT surface, which requires that energy barriers of 2.4 kcal mol^{-1} are surmounted. The transition states of the rearrangement process correspond to the ethene–methylene π complexes at $\tau_1 = 60°$, 180°, and 300°.

If radical cation **1** follows the dotted minimum-energy path on the JT surface, it undergoes the process of bond pseudorotation. In Fig. 2, bond pseudorotation is illustrated by following the long (red) CC bond in the biradicaloid form at $\tau_1 = 0°$ along the pseudorotation path. To identify its position in the three-membered ring, C atom 1 is indicated by a black dot. For a complete pseudorotation cycle, the red bond rotates once around the periphery of the three-membered ring without generating an angular momentum. This becomes possible because of bond switching events at $\tau_1 = 60°$, 180°, and 300°, which are the locations of the ethene–methylene π-complexes. In these forms, there are two long CC interactions so that the red target bond can switch from one side to the other of the ring (see Figs 2, 4).

Of course, the rotation of the red target bond involves a similar rotation of all ring bonds and therefore the term bond pseudorotation has been coined. By following the movement of the atoms, it can easily be shown that bond pseudorotation is a result of the rotation of all C atoms around positions they would take in the D_{3h}-symmetrical form, i.e. in the 3-gon. The rotations are phase-shifted by 120° and are characterized by a rotation radius directly related to the deformation amplitude t_1.

The energy change along the bond pseudorotation path is small, which means that pseudorotation is a rapid process at room temperature. The energy change along the path can be easily analysed using the deformation coordinates. In Fig. 5, the total deformation amplitude T along the bond pseudorotation path is given as a function of the deformation phase angle τ_1. A large T value implies a strong JT-distortion and thereby also a strong stabilization of the three-membered ring. The T value of the biradicaloid forms at $\tau_1 = 0°$, 120°, and 240° is the largest ($T = 0.15$ Å, MR-AQCC value, Table 1) found along the bond pseudorotation path because these forms can distort by only lengthening one CC bond whereas in the ethene–methylene π-complex, two CC interactions have to be weakened, which limits the overall deformation because it can easily lead to fragmentation of the radical cation **1**.

*Monofluorocyclopropane Radical Cation (**2**)*

Radical cation **2** is not a JT system because its ground state is not degenerate. However, in a hypothetical reference form with a D_{3h}-symmetrical C_3 ring, the $^2A''$ ground state can interact with a low-lying excited state via vibronic coupling involving either an a′- or a″-symmetrical vibrational mode or a linear combination of these modes. In short, an $(A' + A'') \otimes (a' + a'')$ interaction leads to a distortion of the molecular geometry because of a PJTE. This vibronic coupling mechanism is relevant for the whole PJT surface and determines the relative energies of the various forms of **2**. The calculated PJT surface is shown in Fig. 6 in the form of a contour line diagram (top) and a perspective drawing of the three-dimensional surface (bottom).

The energy difference of 16.5 kcal mol^{-1} between the reference form at the origin of the PJT surface and the equilibrium forms of **2** at 119° and 241° provides a qualitative comparison for the degree of PJT stabilization in **2** and JT stabilization in **1** (16.5 vs 20.3 kcal mol^{-1} at the EOMIP-CCSD/cc-pVTZ level). Hence, the JT effect has a larger energetic effect than the PJTE although the two systems are closely related and the deformation amplitudes T at the energy minima (0.140 vs 0.144 Å, Table 1) suggest the larger distortion for the PJT system.

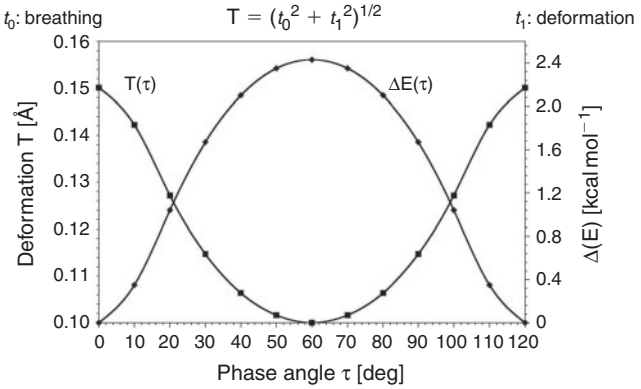

Fig. 5. Variation of the energy change ΔE and the total deformation amplitude T along the bond pseudorotation path on the Jahn–Teller surface (τ_1 from 0° → 360°) of the cyclopropane radical cation **1**. MR-AQCC(5,6)/cc-pVTZ calculations.

The equilibrium geometries of **2** are found for the biradicaloid forms at $\tau_1 = 119°$ and 241° for which the F atom is positioned at one of the terminal C atoms (Fig. 6, Table 1). The latter carry most of the positive charge. F can interact with carbenium atoms by π-donation, thus establishing a CF bond with partial double-bond character.[20] This leads to an overall stabilization of the radical cation located at the two energy minima at 119° and 241° (see lower part of Fig. 6). A path of minimum energy connects these minima on the PJT surface. The barrier to interconversion is 2.2 kcal mol^{-1} where the ethene–fluoromethylene–π complex is positioned at the transition state (TS) of this process. At low temperatures, rapid interconversion of the biradicaloid forms at 119° and 241° is possible, whereas bond pseudorotation should take place only at room temperature because of a relatively high energy barrier of 12.0 kcal mol^{-1}.

In physics, an incomplete rotation is called a libration. Therefore, we call the interconversion between the biradicaloid forms at 119° and 241° a bond pseudolibration, which at low

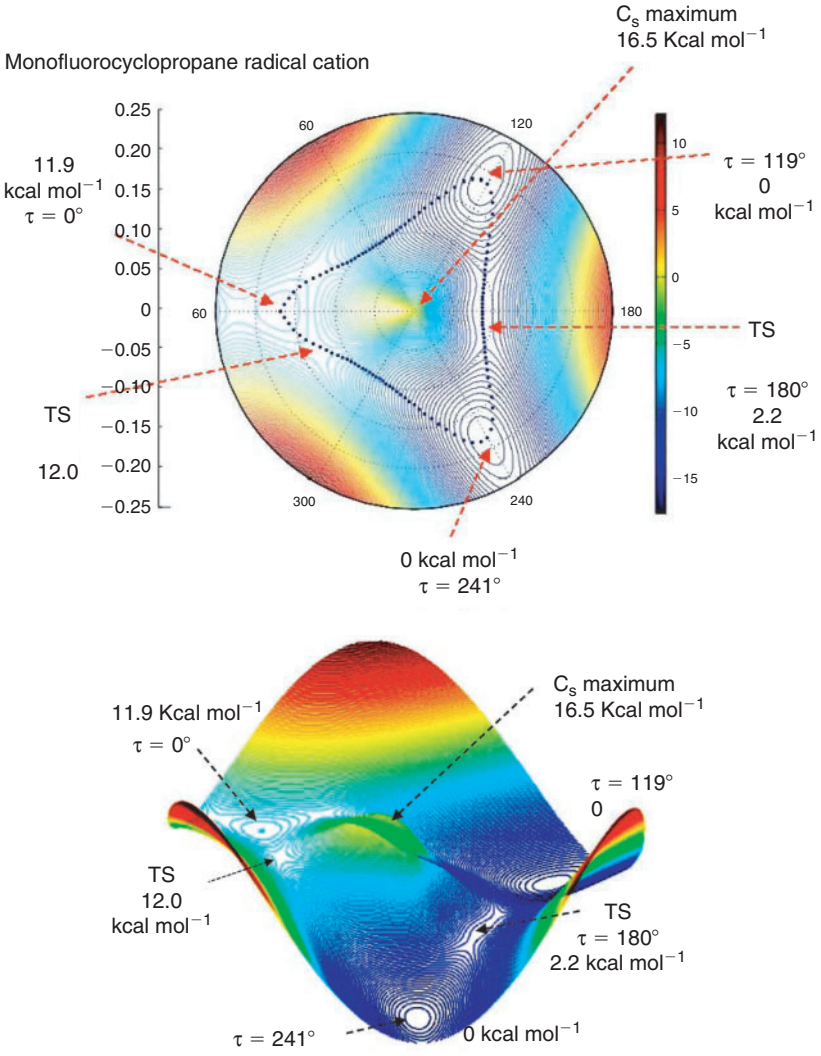

Fig. 6. Pseudo-Jahn–Teller (PJT) surface of the monofluorocyclopropane radical cation **2**. Top: contourline diagram. Bottom: perspective drawing of the PJT surface. The small changes in t_0 are not considered.

temperatures will be the dominant rearrangement process. With increasing temperature, it can extend to a complete bond pseudorotation along the dotted path in Fig. 6. The bond pseudorotation path has to pass a high-lying energy plateau of 12 kcal mol^{-1}, which is populated by slightly distorted biradicaloid forms with F at the central rather than the terminal C atoms (see Fig. 2; there, the long CC interaction of the biradicaloid forms at $\tau_1 = 0°, 120°, 240°$ is given in red). On the energy plateau, there is a flat energy minimum at $\tau_1 = 0°$ and $t_1 = 0.147$ Å, which is 11.9 kcal mol^{-1} above the global minima. The local minimum is separated from the lower-lying energy regions by two TSs at 15° and 345° by a barrier of just 0.1 kcal mol^{-1}.

The central energy mountain of 16.5 kcal mol^{-1} makes a ring interconversion from 0° to 180° at lower temperatures similarly as unlikely as the bond pseudorotation process. At room temperature, the direct interconversion from 0° to 180° becomes possible. As this rearrangement resembles an inversion of puckered ring conformations through a planar ring (the planar ring is a reference form as in the D_{3h}-symmetrical C_3 ring in the case of **1** and **2**), we call the interconversion from 0° to 180° a ring pseudoinversion. This process can also be viewed as bond-stretch isomerism between the forms at 0° to 180° because a short(er) and a long(er) bond are pairwise interconverted. Furthermore, it has to be noted that the ring pseudoinversion path after passing the maximum at $t_1 = 0°$ has a valley-ridge inflection point at which two side paths develop that lead directly to the global minima at 119° and 241°. In the perspective drawing of the three-dimensional PJT surface of Fig. 6, the ridge path down to the TS at $\tau_1 = 180°$ is clearly visible, i.e. the TS of bond pseudolibration is a bifurcation point of the ring pseudoinversion path.

The PJT energies of **2** are strongly affected by the CF bond-stabilization effect. This is illustrated in Fig. 7 where the changes of the CF bond length along the bond pseudorotation path are plotted as a function of the deformation phase angle τ_1. For τ_1 values close to 0°, there is no CF π-delocalization from F to C (C has only little positive charge) and therefore the CF bond is long (EOMIP-CCSD: 1.327 Å, Fig. 1; UB3LYP: 1.339 Å, Fig. 7). At 119° and 241°, the CF partial double-bond character is most strongly developed, thus leading to the shortest CF bonds (1.284 Å). Positive charge is also found for the methylene group in the ethene–methylene π-complex at 180°. However, both the charge value and the partial CF double-bond character are less developed and therefore a somewhat longer CF bond results (1.286 Å), which is in line with the energy increase of 2.2 kcal mol^{-1}.

It is tempting to explain the relative energies of different forms of **2** exclusively by the partial double-bond character of the CF group. However, it has to be emphasized that the deformation of the radical cation is caused by the PJTE, which is the consequence of a low-lying excited state interacting via vibronic coupling with the ground state. The vibronic coupling mechanism involves not only ring but also substituent vibrations, i.e. the $a' + a''$-symmetrical CF vibrational modes also contribute to the PJTE. We have shown in recent work that the locations of the ring substituents can be expressed in terms of curvilinear coordinates and that any change in the substituent positions in the course of the PJTE is sensitively registered by the latter.[7] For example, the a'-symmetrical CF stretching vibration makes a contribution to the PJTE at 180° rather than at 0°. Hence, the PJTE is the actual cause for ring deformation and charge distribution, which in consequence can lead to the development of partial π character of the CF bond.

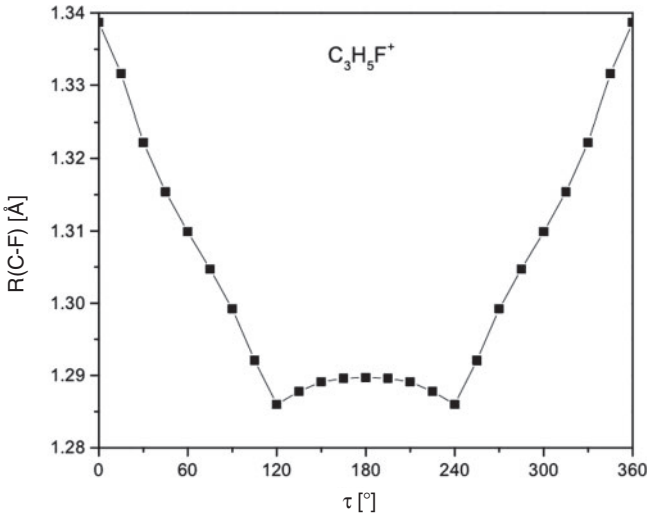

Fig. 7. Change of the CF bond length of **2** along the bond pseudorotation path.

So far, our analysis of the PJT-distortions of **2** focussed on the PJT energy surface, which changes to an enthalpy surface if vibrational and thermochemical corrections are included. Clearly, in such a situation, the minimum at $\tau_1 = 0°$ vanishes (as verified in this work by vibrational frequency calculations at the DFT level) and a single TS at $\tau_1 = 0°$ develops. There is still a bond pseudorotation path leading up a valley to an enthalpy plateau at $\tau_1 = 0 \pm 20°$. The topology of the PJT surface does not change and the same dynamic processes as discussed above take place on the PJT enthalpy surface.

*Pentafluoro Cyclopropane Radical Cation (**3**)*

The PJT surface of **3** differs significantly from that of **2** in so far as the relative energies are reversed and the bond pseudorotation path has a much larger variation in t_1 (see Fig. 8). The most stable form is found for $\tau_1 = 0°$ and $t_1 = 0.214$ Å (Table 1, Fig. 1). In this geometry, the H atom is located at the central atom, i.e. four of the five F atoms are positioned at the positively charged terminal C atoms and therefore establish CF bonds with partial π character (1.267 and 1.270 Å; see Fig. 1), which leads to an overall stabilization of the radical cation **3**.

There are local minima at $\tau_1 = 119°$ and 241°, with the H atom in one of the positions at the terminal C atoms of the biradicaloid form. The EOMIP-CCSD energy of these forms is 5.0 kcal mol^{-1} relative to that of the global minimum at $\tau_1 = 0°$ and separated from the latter by energy barriers of 11.1 kcal mol^{-1}, which are located at $\tau_1 = 81°$ and 279° ($t_1 = 0.109$ Å). The barrier between the local minima at $\tau_1 = 119°$ and 241° is 16.3 kcal mol^{-1} and located at $\tau_1 = 180°$ ($t_1 = 0.104$ Å). The barrier for ring pseudoinversion is 21.7 kcal mol^{-1} and by this comparable with that of **1**.

At reduced temperatures, radical cation **3** can undergo bond pseudolibration involving the three minimum structures and requiring to pass barriers of 11.1 kcal mol^{-1} at $\tau_1 = 81°$ and 279°. At somewhat higher temperatures, bond pseudorotation becomes possible (barrier: 16.3 kcal mol^{-1}), and at room temperatures, even the crossing of the central maximum (21.7 kcal mol^{-1}) in the form of a ring pseudoinversion can no longer be excluded. In this regard, the dynamic processes in **2** and **3** are similar although there are differences in the details.

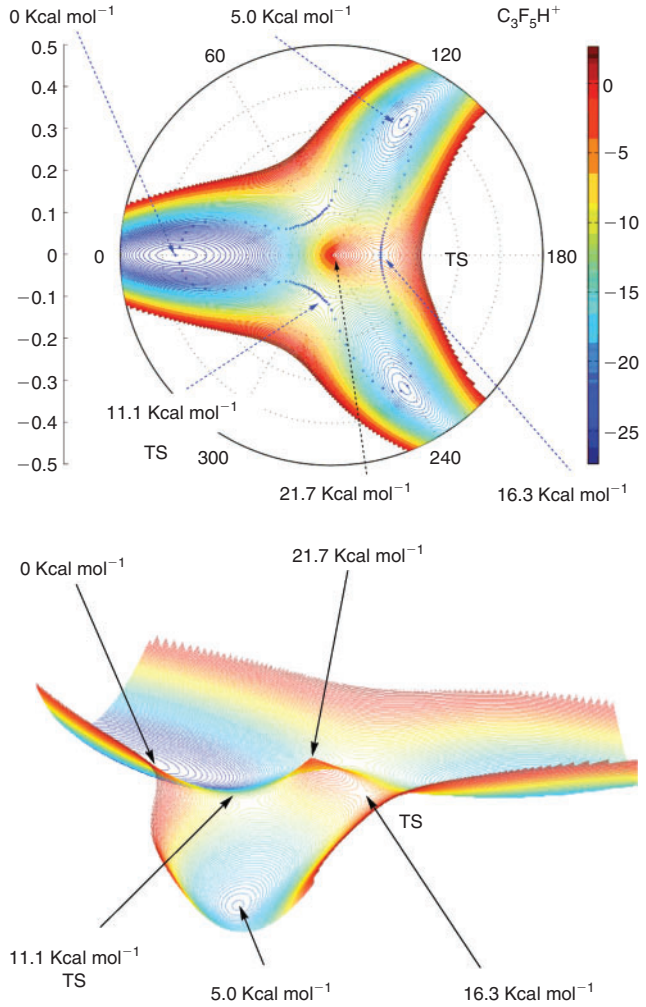

Fig. 8. Pseudo-Jahn–Teller (PJT) surface of the pentafluorocyclopropane cation **3**. Top: contourline diagram. Bottom: perspective drawing of the PJT surface. The small changes in t_0 are not considered.

The bond pseudorotation path of radical cation **3** is strongly curved, which is reflected by the total deformation amplitudes T (variation between 0.105 and 0.284 Å; see Table 1) and which is three times as large as that calculated for **2** and four times as large as that for **1**. Accordingly, the CC interaction distances of **3** vary between 1.436 and 2.163 Å. We note that the atoms make a similar movement when circling around their fixed points. The strong curving of the bond pseudorotation path is a direct result of the pentafluorination of the radical cation and reveals that the electronic structure changes in **3** are larger during bond pseudorotation than in **1** and **2**.

The biradicaloid forms can widen the C···C up to the breaking point (the C···C distances obtained are typical of TS distances for CC bond formation or cleavage). However, in the cases of the π-complex forms at $\tau_1 = 81°$, 180°, or 279°, any larger deformation will lead to dissociation by removing the CHF or CF_2 group from the ethene basis. In this connection, it is interesting to note that the biradicaloid minima are located in flat valleys extending radially to larger T values (see Fig. 8). This indicates that the biradicaloid forms can carry out a large-amplitude C···C stretching vibrations.

If four electronegative F atoms are bonded to the terminal C atoms of the biradicaloid form, hybridization partly converts from sp^3 into $sp^2\pi$ to increase the π interactions between C and the F atoms. Consequently, the bonding interactions between the terminal C atoms become much weaker and the weakening is enhanced by exchange repulsion between the terminal F atoms. The ring of **3** opens, which is reflected by a C2C3 distance of 2.012 Å compared with values of 1.825 and 1.837 Å in the case of **1** and **2** respectively ($\tau_1 = 0°$, see Fig. 1).

Noteworthy is that DFT as the method, which includes far fewer non-dynamic electron correlation effects, leads to much larger deformations of the three cyclopropane radical cations, which confirms how important the use of multireference methods is to obtain a reliable description of the JT or PJT surfaces.

Radical cation **3** in its equilibrium geometry is best described as a biradical cation with trimethylene character. It has to be noted that so far experimentalists have unsuccessfully searched for a trimethylene radical cation. Perfluorinated or strongly fluorinated radical cations such as **3** seem to be promising candidates for realizing an F-substituted trimethylene radical cation. Molecule **3** is more stable than radical cations **1** and **2** because it has four F atoms in the terminal positions of the biradicaloid form corresponding to the equilibrium energy. This can be illustrated by the following formal reaction:

$$4 \times C_3H_6^{+\cdot} + C_3F_5H^{+\cdot} \longrightarrow 5 \times C_3FH_5^{+\cdot} \quad -25.40\,\text{kcal mol}^{-1}$$

which is exothermic by 25.40 kcal mol^{-1}. Obviously, the CF stabilization in five molecules of **2** determines the exothermicity of this reaction. In the equilibrium geometry of **3**, only four F atoms can take such an optimal position. Of course, this implies that five molecules of **2** are needed to outweigh the stability of **3** where it is assumed that **1**, which does not benefit from any partial CF double bond character, is the least stable radical cation.

Conclusions

Curvilinear coordinates are very well suited for describing the geometry of ring molecules and spanning a (2N – 3)-dimensional JT or PJT surface. They define the molecular geometry without ever referring to bond lengths and bond angles. The curvilinear coordinates used in this work form of a set of 2N – 4 deformation amplitudes and deformation phase angles, which were used to describe JT and PJT deformations of cyclopropane radical cations. We have derived them in such a way that geometry optimization and vibrational frequency calculations can be carried out without referring to internal coordinates. For three-membered ring systems such as **1**, **2**, and **3**, the curvilinear coordinates are t_0 (related to the breathing radius R), t_1, and τ_1. The deformation amplitudes t_0 and t_1 are used to define the total deformation amplitude T that gives a direct quantitative measure of the extent of JT- or PJT-distortion.

1. A large total deformation amplitude T indicates a large PJT deformation and thereby a large stabilization relative to a reference form with a D_{3h}-symmetrical three-membered ring. The analysis of JT- or PJT-distortions in terms of internal coordinates is difficult and in most cases not conclusive. However, the analysis based on curvilinear coordinates tremendously facilitates the understanding of structure and stability of JT- or PJT-distorted forms.
2. The cyclopropane radical cation **1** is a JT-unstable system that deforms to C_{2v}- and C_s-symmetrical forms filling a two-dimensional JT space spanned by the deformation amplitude t_1 and the deformation phase angle τ_1. Radical cation **1** undergoes bond pseudorotation on the JT surface surmounting a barrier of just 2.1 kcal mol^{-1}.

3. The dynamic process of bond pseudorotation involves the rotation of all ring bonds around the periphery of the ring (see Fig. 2). Bond pseudorotation is the result of the fact that all ring atoms rotate around fixed points given by a 3-gon with a radius depending on t_1 and the rotation of different atoms being phase-shifted by an angle of $360/3 = 120°$.
4. The energy change of **1** along the bond pseudorotation path is a function of the total deformation amplitude T. The biradicaloid forms can lead to larger T values because only one of the three CC interactions is weakened whereas for the ethene–methylene π-complex forms, two CC interactions are weakened, which limits the magnitude of the deformation given by T.
5. For the two F-substituted cyclopropane radical cations **2** and **3**, the PJTE, corresponding to an $(A' + A'') \otimes (a' + a'')$ interaction, determines structure and stability. The PJT surfaces obtained for the two radical cations differ significantly from the JT surface of the parent radical cation and from each other, thus reflecting the different impact of the fluoro substituents.
6. Two new dynamic processes are described for the F-substituted radical cations: (i) bond pseudolibration is an incomplete bond pseudorotation process, which takes place at lower temperatures and is only hindered by relatively small barriers (**2**, 2.2 kcal mol^{-1}; **3**, 11.1 kcal mol^{-1}); and (ii) ring pseudoinversion is a dynamic process of relatively high energy and implies that the molecule crosses the central maximum (**2**, 16.5 kcal mol^{-1}; **3**, 21.7 kcal mol^{-1}).
7. At room temperature, **2** and **3** will undergo both bond pseudorotation (barriers: 12.0 and 16.3 kcal mol^{-1}) and ring pseudoinversion, i.e. the PJT surfaces of **2** and **3** (Figs 6, 8) will be populated according to a Boltzmann distribution. In this way, averaged molecular properties can be determined and compared with experimental results.[21]
8. Energy trends in **2** and **3** can be easily explained considering the distribution of the positive charge among the three C atoms in the biradicaloid and ethene–methylene π-complex forms and the positions of the CF bonds. If F is bonded to a strongly charged centre, π donation from F to C will lead to partial double-bond character and an overall stabilization of the ring system. The more such CF partial double bonds are established, the more stable is the ring configuration in question.
9. Penta- and perfluorocyclopropane radical cations possess the structure of a trimethylene radical cation. In future work, we will study their reactions.

References

[1] A. D. Liehr, *J. Phys. Chem.* **1963**, *67*, 389. doi:10.1021/J100796A043
[2] A. D. Liehr, *J. Phys. Chem.* **1963**, *67*, 472.
[3] I. B. Bersuker, *The Jahn–Teller Effect* **2006** (Cambridge University Press: Cambridge, UK).
[4] I. B. Bersuker, *Chem. Rev.* **2013**, *113*, 1351. doi:10.1021/CR300279N
[5] D. Cremer, E. Kraka, K. J. Szabo, in *The Chemistry of Functional Groups*, *The Chemistry of the Cyclopropyl Group* (Ed. Z. Rappoport) **1995**, Vol. 2, p. 43 (John Wiley: New York).
[6] W. Zou, D. Izotov, D. Cremer, *J. Phys. Chem.* **2011**, *115*, 8731. doi:10.1021/JP2041907
[7] W. Zou, M. Filatov, D. Cremer, *Int. J. Quantum Chem.* **2012**, *112*, 3277. doi:10.1002/QUA.24116
[8] D. Cremer, D. Izotov, W. Zou, E. Kraka, *RING, a Coordinate Transformation Program* **2011** (Southern Methodist University: Dallas, TX).
[9] E. Kraka, M. Filatov, W. Zou, J. Gräfenstein, D. Izotov, J. Gauss, Y. He, A. Wu, vs Polo, L. Olsson, Z. Konkoli, Z. He, D. Cremer, *COLOGNE2013* **2013** (Southern Methodist University: Dallas, TX).
[10] A. D. Becke, *J. Chem. Phys.* **1993**, *98*, 5648. doi:10.1063/1.464913
[11] P. J. Stephens, F. J. Devlin, C. F. Chablowski, M. J. Frisch, *J. Phys. Chem.* **1994**, *98*, 11623. doi:10.1021/J100096A001
[12] T. H. Dunning, *J. Chem. Phys.* **1989**, *90*, 1007. doi:10.1063/1.456153
[13] K. Raghavachari, G. W. Trucks, J. A. Pople, M. Head-Gordon, *Chem. Phys. Lett.* **1989**, *157*, 479. doi:10.1016/S0009-2614(89)87395-6
[14] P. G. Szalay, R. J. Bartlett, *Chem. Phys. Lett.* **1993**, *214*, 481. doi:10.1016/0009-2614(93)85670-J
[15] M. Nooijen, J. G. Snijders, *Int. J. Quantum Chem. Quantum Chem. Symp.* **1992**, *26*, 55.
[16] M. Nooijen, J. G. Snijders, *Int. J. Quantum Chem.* **1993**, *48*, 15. doi:10.1002/QUA.560480103
[17] J. F. Stanton, J. Gauss, *J. Chem. Phys.* **1994**, *101*, 8938. doi:10.1063/1.468022
[18] J. F. Stanton, J. Gauss, M. E. Harding, P. G. Szalay, with contributions from A. A. Auer, R. J. Bartlett, U. Benedikt, C. Berger, D. E. Bernholdt, Y. J. Bomble, L. Cheng, O. Christiansen, M. Heckert, O. Heun, C. Huber, T.-C. Jagau, D. Jonsson, J. Jusélius, K. Klein, W. J. Lauderdale, D. A. Matthews, T. Metzroth, L. A. Mück, D. P. O′Neill, D. R. Price, E. Prochnow, C. Puzzarini, K. Ruud, F. Schiffmann, W. Schwalbach, S. Stopkowicz, A. Tajti, J. Vázquez, F. Wang, J. D. Watts, *CFOUR, a Quantum Chemical Program Package* **2010** (J. F. Stanton: Austin, TX). Available at http://www.cfour.de (accessed 14 November 2013).
[19] H. J. Werner, P. J. Knowles, G. Kniza, F. R. Manby, M. Schütz, P. Celani, T. Korona, R. Lindh, A. Mitrushenkov, G. Rauhut, K. R. Shamasundar, T. B. Adler, R. D. Amos, A. Bernhardsson, A. Berning, D. L. Cooper, M. J. O. Deegan, A. J. Dobbyn, F. Eckert, E. Goll, C. Hampel, A. Hesselmann, G. Hetzer, T. Hrenar, G. Jansen, C. Köppl, Y. Liu, A. W. Lloyd, R. A. Mata, A. J. May, S. J. McNicholas, W. Meyer, M. E. Mura, A. Nicklass, D. P. O′Neill, P. Palmieri, K. Pflüger, R. Pitzer, M. Reiher, T. Shiozaki, H. Stoll, A. J. Stone, R. Tarroni, T. Thorsteinsson, M. Wang, A. Wolf, *MOLPRO, Version 2010.1, a Package of Ab Initio Programs* **2010** (H.-J. Werner: Stuttgart). Available at http://www.cfour.de (accessed 14 November 2013).
[20] E. Kraka, D. Cremer, *ChemPhysChem* **2009**, *10*, 686. doi:10.1002/CPHC.200800699
[21] A. Wu, D. Cremer, *J. Phys. Chem. A* **2003**, *107*, 1797. doi:10.1021/JP022277M